

10–13 Oct. GSA Connects 2021

# GSA TODAY

 THE GEOLOGICAL SOCIETY  
OF AMERICA®

VOL. 31, NO. 5 | MAY 2021

## **Curation and Analysis of Global Sedimentary Geochemical Data to Inform Earth History**



# Curation and Analysis of Global Sedimentary Geochemical Data to Inform Earth History

**Akshay Mehra\***, Dartmouth College, Dept. of Earth Sciences, Hanover, New Hampshire 03755, USA; **C. Brenhin Keller**, Dartmouth College, Dept. of Earth Sciences, Hanover, New Hampshire 03755, USA; **Tianran Zhang**, Dept. of Earth Sciences, Dartmouth College, Hanover, New Hampshire 03755, USA; **Nicholas J. Tosca**, Dept. of Earth Sciences, University of Cambridge, Cambridge CB2 1TN, UK; **Scott M. McLennan**, State University of New York, Stony Brook, New York 11794, USA; **Erik Sperling**, Dept. of Geological Sciences, Stanford University, Stanford, California 94305, USA; **Una Farrell**, Dept. of Geology, Trinity College Dublin, Dublin, Ireland; **Jochen Brocks**, Research School of Earth Sciences, Australian National University, Canberra, Australia; **Donald Canfield**, Nordic Center for Earth Evolution (NordCEE), University of Southern Denmark, Denmark; **Devon Cole**, School of Earth and Atmospheric Science, Georgia Institute of Technology, Atlanta, Georgia 30332, USA; **Peter Crockford**, Earth and Planetary Science, Weizmann Institute of Science, Rehovot, Israel; **Huan Cui**, Equipe Géomicrobiologie, Université de Paris, Institut de Physique, Paris, France, and Dept. of Earth Sciences, University of Toronto, Ontario M5S, Canada; **Tais W. Dahl**, GLOBE Institute, University of Denmark, Copenhagen, Denmark; **Keith Dewing**, Natural Resources Canada, Geological Survey of Canada, Calgary, Ontario T2L 2A7, Canada; **Joseph F. Emmings**, British Geological Survey, Nicker Hill, Keyworth, Nottingham NG12 5GG, UK; **Robert R. Gaines**, Dept. of Geology, Pomona College, Claremont, California 91711, USA; **Tim Gibson**, Dept. of Earth & Planetary Sciences, Yale University, New Haven, Connecticut 06520, USA; **Geoffrey J. Gilleaudeau**, Atmospheric, Oceanic, and Earth Sciences, George Mason University, Fairfax, Virginia 22030, USA; **Romain Guilbaud**, Géosciences Environnement Toulouse, CNRS, Toulouse, France; **Malcom Hodgskiss**, Dept. of Geological Sciences, Stanford University, Stanford, California 94305, USA; **Amber Jarrett**, Onshore Energy Directorate, Geoscience Australia, Australia; **Pavel Kabanov**, Natural Resources Canada, Geological Survey of Canada, Calgary T2L 2A7, Canada; **Marcus Kunzmann**, Mineral Resources, CSIRO, Kensington, Australia; **Chao Li**, State Key Laboratory of Biogeology and Environmental Geology, China University of Geosciences, Wuhan, China; **David K. Loydell**, School of the Environment, Geography and Geosciences, University of Portsmouth, Portsmouth PO1 2UP, UK; **Xinze Lu**, Dept. of Earth and Environmental Sciences, University of Waterloo, Waterloo N2L 3G1, Canada; **Austin Miller**, Dept. of Earth and Environmental Sciences, University of Waterloo, Waterloo N2L 3G1, Canada; **N. Tanner Mills**, Dept. of Geology and Geophysics, Texas A&M University, College Station, Texas 77843, USA; **Lucas D. Mouro**, Geology Dept., Federal University of Santa Catarina, Santa Catarina State, Brazil; **Brennan O'Connell**, School of Earth Sciences, University of Melbourne, Melbourne, Australia; **Shanan E. Peters**, Dept. of Geoscience, University of Wisconsin–Madison, Madison 53706, Wisconsin, USA; **Simon Poulton**, School of Earth and Environment, University of Leeds, Leeds LS2 9JT, UK; **Samantha R. Ritzer**, Dept. of Geological Sciences, Stanford University, Stanford, California 94305, USA; **Emmy Smith**, Dept. of Earth and Planetary Sciences, Johns Hopkins University, Baltimore, Maryland 21218, USA; **Philip Wilby**, British Geological Survey, Nicker Hill, Keyworth, Nottingham NG12 5GG, UK; **Christina Woltz**, Dept. of Earth Science, University of California, Santa Barbara, California 93106, USA; **Justin V. Strauss**, Dept. of Earth Sciences, Dartmouth College, Hanover, New Hampshire 03755, USA

## ABSTRACT

Large datasets increasingly provide critical insights into crustal and surface processes on Earth. These data come in the form of published and contributed observations, which often include associated metadata. Even in the best-case scenario of a carefully curated dataset, it may be non-trivial to extract meaningful analyses from such compilations, and choices made with respect to filtering, resampling, and averaging can affect the resulting trends and any interpretation(s) thereof. As a result, a thorough understanding of how to digest, process, and analyze large data compilations is required. Here, we present a generalizable

workflow developed using the Sedimentary Geochemistry and Paleoenvironments Project database. We demonstrate the effects of filtering and weighted resampling on  $Al_2O_3$  and U contents, two representative geochemical components of interest in sedimentary geochemistry (one major and one trace element, respectively). Through our analyses, we highlight several methodological challenges in a “bigger data” approach to Earth science. We suggest that, with slight modifications to our workflow, researchers can confidently use large collections of observations to gain new insights into processes that have shaped Earth’s crustal and surface environments.

## INTRODUCTION

The study of Earth’s past relies on a record that is spatially and temporally variable and, by some metrics, woefully undersampled. Through every geochemical analysis, fossil identification, and measured stratigraphic section, Earth scientists continuously add to this historical record. Compilations of such observations can illuminate global trends through time, providing researchers with crucial insights into our planet’s geological and biological evolution. These compilations can vary in size and scope, from hundreds of manually curated entries in a spreadsheet to millions of records stored in software databases. The latter form is exemplified by

databases such as The Paleobiology Database (PBDB; Peters and McClennen, 2016), Macrostrat (Peters et al., 2018), EarthChem (Walker et al., 2005), Georoc (Sarbas, 2008), and the Sedimentary Geochemistry and Paleoenvironments Project (SGP, this study).

Of course, large amounts of data are not new to the Earth sciences, and, with respect to volume, many Earth history and geochemistry compilations are small in comparison to the datasets used in other subdisciplines, including seismology (e.g., Nolet, 2012), climate science (e.g., Faghmous and Kumar, 2014), and hydrology (e.g., Chen and Wang, 2018). As a result, many Earth history compilations likely do not meet the criteria to be called “big data,” which is a term that describes very large amounts of information that accumulate rapidly and which are heterogeneous and unstructured in form (Gandomi and Haider, 2015; or “if it fits in memory, it is small data”). That said, the tens of thousands to millions of entries present in such datasets do represent a new frontier for those interested in our planet’s past. For many Earth historians, however, and especially for geochemists (where most of the field’s efforts traditionally have focused on analytical measurements rather than data analysis; see Sperling et al., 2019), this frontier requires new outlooks and toolkits.

When using compilations to extract global trends through time, it is important to recognize that large datasets can have several inherent issues. Observations may be unevenly distributed temporally and/or spatially, with large stretches of time (e.g., parts of the Archean Eon) or space (e.g., much of Africa; Fig. S1<sup>1</sup>) lacking data. There may also be errors with entries—mis-labeled values, transposition issues, and missing metadata can occur in even the most carefully curated compilations. Even if data are pristine, they may span decades of acquisition with evolving techniques, such that both analytical precision and measurement uncertainty are non-uniform across the dataset (Fig. S2 [see footnote 1]). Careful examination may demonstrate that contemporaneous and co-located observations do not agree. Additionally, data often are not targeted, such that not every entry may be necessary for (or even useful to) answering a particular question.

Luckily, these (and other) issues can be addressed through careful processing and analysis, using well-established statistical and computational techniques. Although such techniques have complications of their own (e.g., a high degree of comfort with programming often is required to run code efficiently), they do provide a way to extract meaningful trends from large datasets. No one lab can generate enough data to cover Earth’s history densely enough (i.e., in time and space), but by leveraging compilations of accumulated knowledge, and using a well-developed computational pipeline, researchers can begin to ascertain a clearer picture of Earth’s past.

### A PROPOSED WORKFLOW

The process of transforming entries in a dataset into meaningful trends requires a series of steps, many with some degree of user decision making. Our proposed workflow is designed with the express intent of removing unfit data while appropriately propagating uncertainties. First, a compiled dataset is made or sourced (Fig. S3, i. [see footnote 1]). Next, a researcher chooses between in-database analysis and extracting data into another format, such as a text file (Fig. S3, ii). This choice does nothing to the underlying data—its sole function is to recast information into a digital format that the researcher is most comfortable with. Then, a decision must be made about whether to remove entries that are not pertinent to the question at hand (Fig. S3, iii). Using one or more metadata parameters (e.g., in the case of rocks, lithological descriptions), researchers can turn large compilations into targeted datasets, which then can be used to answer specific questions without the influence of irrelevant data. Following this gross filtering, researchers must decide between removing outliers or keeping them in the dataset (Fig. S3, iv). Outliers have the potential to drastically skew results in misleading ways. Ascertaining which values are outliers is a non-trivial task, and all choices about outlier exclusion must be clearly described when presenting results. Finally, samples are drawn from the filtered dataset (i.e., “resampling”) using a weighting scheme that seeks to address the spatial and temporal heterogeneities—as well as analytical uncertainties—of

the data (Fig. S3, vi). To calculate statistics from the data, multiple iterations of resampling are required.

### CASE STUDY: THE SEDIMENTARY GEOCHEMISTRY AND PALEOENVIRONMENTS PROJECT

The SGP project seeks to compile sedimentary geochemical data, made up of various analytes (i.e., components that have been analyzed), from throughout geologic time. We applied our workflow to the SGP database<sup>2</sup> to extract coherent temporal trends in Al<sub>2</sub>O<sub>3</sub> and U from siliciclastic mudstones. Al<sub>2</sub>O<sub>3</sub> is relatively immobile and thus useful for constraining both the provenance and chemical weathering history of ancient sedimentary deposits (Young and Nesbitt, 1998). Conversely, U is highly sensitive to redox processes. In marine mudstones, U serves as both a local proxy for reducing conditions in the overlying water column (i.e., authigenic U enrichments only occur under low-oxygen or anoxic conditions and/or very low sedimentation rates; see Algeo and Li, 2020) and a global proxy for the areal extent of reducing conditions (i.e., the magnitude of authigenic enrichments scales in part with the global redox landscape; see Partin et al., 2013).

SGP data are stored in a PostgreSQL relational database that currently comprises a total of 82,579 samples (Fig. 1). The SGP database was created by merging sample data and geological context information from three separate sources, each with different foci and methods for obtaining the “best guess” age of a sample (i.e., the interpreted age as well as potential maximum and minimum ages). The first source is direct entry by SGP team members, which focuses primarily on Neoproterozoic–Paleozoic shale samples and has global coverage. Due to the direct involvement of researchers intimately familiar with their sample sets, these data have the most precise (Fig. 1A)—and likely also most accurate—age constraints. Second, the SGP database has incorporated sedimentary geochemical data from the United States Geological Survey (USGS) National Geochemical Database (NGDB), comprising samples from projects completed between the 1960s and 1990s. These samples, which

<sup>1</sup>Supplemental Material: table of valid lithologies; map depicting sample locations; crossplot illustrating analytical uncertainty; flowchart of the proposed workflow; histograms showing the effects of progressive filtering, the distribution of spatial and age scales, and proximity and probability values; and results of sensitivity tests. Go to <https://doi.org/10.1130/GSAT.S.14179976> to access the supplemental material; contact [editing@geosociety.org](mailto:editing@geosociety.org) with any questions.

<sup>2</sup>All code used in this study is located at <https://github.com/akshaymehra/dataCompilationWorkflow>.

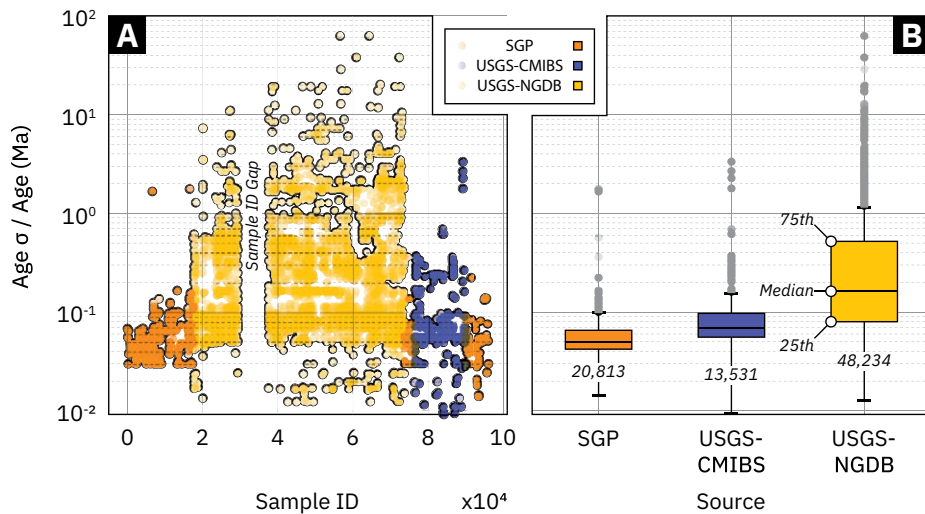


**Figure 1. Visualizations of data in the Sedimentary Geochemistry and Paleoenvironments Project (SGP) database. (A) Relative age uncertainty (i.e., the reported age  $\sigma$  divided by the reported interpreted age) versus Sample ID. The large gap in Sample ID values resulted from the deletion of entries during the initial database compilation and has no impact on analyses. (B) Box plot showing the distributions of relative ages with respect to the sources of data. CMIBS—Critical Metals in Black Shales; NGDB—National Geochemical Database.**

cover all lithologies and are almost entirely from Phanerozoic sedimentary deposits of the United States, are associated with the continuous-time age model from Macrostrat (Peters et al., 2018). Finally, the SGP database includes data from the USGS Global Geochemical Database for Critical Metals in Black Shales project (CMIBS; Granitto et al., 2017), culled to remove ore-deposit related samples. The CMIBS samples predominantly are shales, have global coverage, and span the entirety of Earth's sedimentary record. When possible, the CMIBS data are associated with Macrostrat continuous-time age models; otherwise, the data are assigned age information by SGP team members (albeit without detailed knowledge of regional geology or geologic units).

### Cleaning and Filtering

We exported SGP data into a comma-separated values (.csv) text file, using a custom structured query language (SQL) query. In the case of geochemical analytes, this query included unit conversions from both weight percent (wt%) and parts per billion (ppb) to parts per million (ppm). After export, we parsed the .csv file and screened the data through a series of steps. First, if multiple values were reported for an analyte in a sample, we calculated and stored the mean (or weighted mean, if there were enough values) and standard deviation of the analyte. Then, we redefined empty values—which are the result of abundance being above or below detection—as “not a number” (NaN, a special

value defined by Institute of Electrical and Electronics Engineers [IEEE] floating-point number standard that always returns false on comparison; see IEEE, 2019). Next, we converted major elements (e.g., those that together comprise >95% of Earth's crust or individually >1 wt% of a sample) into their corresponding oxides; if an oxide field did not already exist, or if there was no measurement for a given oxide, the converted value was inserted into the data structure. Then, we assigned both age and measurement uncertainties to the parsed data. In the case of the parsed SGP data, 5,935 samples (i.e., 7.1% of the original dataset) lacked an interpreted age and so no uncertainty could be assigned. For the remainder, we calculated an initial absolute age uncertainty by either using the reported maximum and minimum ages:

$$\sigma = \frac{|\text{age}_{\text{maximum}} - \text{age}_{\text{minimum}}|}{2},$$

or, if there were no maximum and minimum age values available, by defaulting to a two-sigma value of 6% of the interpreted age:

$$\sigma = 0.03 * \text{age}_{\text{interpreted}}.$$

The choice of a 6% default value was based on a conservative estimate of the precision of common in situ dating techniques (see, for example, Schoene, 2014). Additionally, we enforced a minimum  $\sigma$  of 25 million years:

$$\sigma = \max(\sigma, 25).$$

Effectively, each datum can be thought of as a Gaussian distribution along the time axis with a  $\sigma$  of at least 25 million years (the minimum value of which may be thought of as a kernel bandwidth, rather than an analytical uncertainty). The selection of this  $\sigma$  value should correspond to an estimate of the processes that are being investigated (e.g., tectonic changes in provenance). We did not impose a minimum relative age uncertainty.

With respect to measurement uncertainties, we assigned an absolute uncertainty to every analyte that lacked one by multiplying the reported analyte value by a relative error. In future database projects, there is considerable scope to go beyond this coarse uncertainty quantification strategy. For example, given the detailed metadata associated with each sample in the SGP database, it would be straightforward to develop correction factors or uncertainty estimates for different geochemical methodologies (e.g., inductively coupled plasma–mass spectrometry [ICP-MS] versus inductively coupled plasma–optical emission spectrometry [ICP-OES], benchtop versus handheld X-ray fluorescence spectrometry [XRF], etc.). Correcting data for biases introduced during measurement is common in large Earth science datasets (Chan et al., 2019). However, such corrections previously have not been attempted in sedimentary geochemistry datasets.

Next, we processed the data through a simple lithology filter because, in the general case of rock-based datasets, only lithologies relevant to the question(s) at hand provide meaningful information. The choice of valid lithologies (or, for that matter, any other filterable metadata) are dependent on the researchers' question(s). As highlighted in the Discussion section, lithology filtering has significant implications for redox-sensitive and/or mobile/immobile elements. In this case study, our aim was to only sample data generated from siliciclastic mudstones. To decide which values to screen by, we manually examined a list made up of all unique lithologies in the dataset. We excluded samples that did not match our list of chosen lithologies (removing ~63.5% of the data; Table S1; Fig. S4 [see footnote 1]). Our strategy ensured that we only included mudstones *sensu lato* (see Potter et al., 2005, for a general description) where the lithology was coded. Alternative methods—such as choosing samples based on an Al cutoff value (e.g., Reinhard et al., 2017)—likely would result in a set comprising both mudstone and non-mudstone coded lithologies. In the future,

improved machine learning algorithms, designed to classify unknown samples based on their elemental composition, may provide a more sophisticated means by which to generate the largest possible dataset of lithology-appropriate samples.

We then completed a preliminary screening of the lithology filtered samples by checking if extant analyte values were outside of physically possible bounds (e.g., individual oxides with wt% less than 0 or greater than 100), and, if so, setting them to NaN. Next, to reduce the number of mudstone samples with detrital or authigenic carbonate and phosphatic mineral phases, we excluded samples with greater than 10 wt% Ca and/or more than 1 wt% P<sub>2</sub>O<sub>5</sub> (removing ~66.9% of the remaining data; Fig. S4 [see footnote 1]). Additionally, in order to ensure that our mudstone samples were not subject to secondary enrichment processes, such as ore mineralization, we queried the USGS NGDB to extract the recorded characteristics of every sample with an associated USGS NGDB identifier. We examined these characteristics for the presence of selected strings (i.e., “mineralized,” “mineralization present,” “unknown mineralization,” and “radioactive”) and excluded any sample exhibiting one or more strings. Finally, as there were still several apparent outliers in the dataset, we manually examined the log histograms of each element and oxide of interest. On each histogram, we demarcated the 0.5th and 99.5th percentile bounds of the data, then visually studied those histograms to exclude “outlier populations,” or samples located both well outside those percentile bounds and not part of a continuum of values (removing ~5.7% of the remaining data; Fig. S4). Following these filtering steps, we saved the data in a .csv text file.

### Data Resampling

We implemented resampling based on inverse distance weighting (after Keller and Schoene, 2012), in which samples closer together—that is, with respect to a metric such as age or spatial distance—are considered to be more alike than samples that are further apart. The inverse weighting of an individual point,  $x$ , is based on the basic form:

$$y(x) = \frac{1}{d(x, x_i)^p},$$

where  $d$  is a distance function,  $x_i$  is a second sample, and  $p$ , which is greater than 0, is a

power parameter. In the case of the SGP data, we used two distance functions, spatial ( $s$ ) and temporal ( $t$ ):

$$s = \frac{\text{arcdistance}(x, x_i)}{\text{scale}_{\text{spatial}}},$$

$$t = \frac{|\text{age}(x - x_i)|}{\text{scale}_{\text{age}}},$$

where *arcdistance* refers to the distance between two points on a sphere, *scale<sub>spatial</sub>* refers to a preselected arc distance value (in degrees; Fig. S5, inset [see footnote 1]), and *scale<sub>age</sub>* is a preselected age value (in million years, Ma). In this case study, we chose a *scale<sub>spatial</sub>* of 0.5 degrees and a *scale<sub>age</sub>* of 10 Ma (see below for a discussion about parameter values).

For  $n$  samples, the proximity value  $w$  assigned to each sample  $x$  is:

$$w(x) = \sum_{i=1}^{i=n} \frac{1}{(s^2 + 1)} + \frac{1}{(t^2 + 1)}.$$

Essentially, the proximity value is a summation of the reciprocals of the distance measures made for each pair of the sample and a single other datum from the dataset. Accordingly, samples that are closer to other data in both time and space will have larger  $w$  values than those that are farther away. Note that the additive term of 1 in the denominator establishes a maximum value of 1 for each reciprocal distance measure.

We normalized the generated proximity values (Fig. S6 [see footnote 1]) to produce a probability value  $P$ . This normalization was done such that the median proximity value corresponded to a  $P$  of ~0.20 (i.e., a 1 in 5 chance of being chosen):

$$P(x) = \frac{1}{\left(w(x) * \text{median}\left(\frac{0.20}{w}\right)\right) + 1}.$$

This normalization results in an “inverse proximity weighting,” such that samples that are closer to other data (which have large  $w$  values) end up with a smaller  $P$  value than those that are far away from other samples. Next, we assigned both analytical and temporal uncertainties to each analyte to be resampled. Then, we culled the dataset into an  $m$  by  $n$  matrix, where each row corresponded to a sample and each column to an analyte. We resampled this culled dataset 10,000 times using a

three-step process: (1) we drew samples, using calculated  $P$  values, with replacement (i.e., each draw considered all available samples, regardless of whether a sample had already been drawn); (2) we multiplied the assigned uncertainties discussed above by a random draw from a normal distribution ( $\mu = 0$ ;  $\sigma = 1$ ) to produce an error value; and (3) we added these newly calculated errors to the drawn temporal and analytical values. Finally, we binned and plotted the resampled data.

Naturally, the reader may ask how we chose the values for *scale<sub>age</sub>* and *scale<sub>temporal</sub>* and what, if any, impact those choices had on the final results? Nominally, the values of *scale<sub>age</sub>* and *scale<sub>temporal</sub>* are controlled by the size and age, respectively, of the features that are being sampled. So, in the case of sedimentary rocks, those values should reflect the length scale and duration of a typical sedimentary basin, such that many samples from the same “spatiotemporal” basin have lower  $P$  values than few samples from distinct basins. Of course, it is debatable what “typical” means in the context of sedimentary basins, as both size and age can vary over orders of magnitude (Woodcock, 2004). Given this uncertainty, we subjected the SGP data to a series of sensitivity tests, where we varied both *scale<sub>age</sub>* and *scale<sub>temporal</sub>*, using logarithmically spaced values of each (Fig. S5 [see footnote 1]). While the uncertainty associated with results varied based on the choice of the two parameters, the overall mean values were not appreciably different (Fig. S7 [see footnote 1]).

### RESULTS

To study the impact of our methodology, we present results for two geochemical components, U and Al<sub>2</sub>O<sub>3</sub> (Fig. 2). Contents-wise, the U and Al<sub>2</sub>O<sub>3</sub> data in the SGP database contain extreme outliers. Many of these outliers were removed using the lithology and Ca or P<sub>2</sub>O<sub>5</sub> screening (Figs. 2A and 2C); the final outlier filtering strategy discussed above handled any remaining values of concern. In the case of U, our multi-step filtering reduced the range of concentrations by three orders of magnitude, from 0–500,000 ppm to 0–500 ppm.

### DISCUSSION

The illustrative examples we have presented have implications for understanding Earth’s history. Al<sub>2</sub>O<sub>3</sub> contents of ancient mudstones appear relatively stable over the

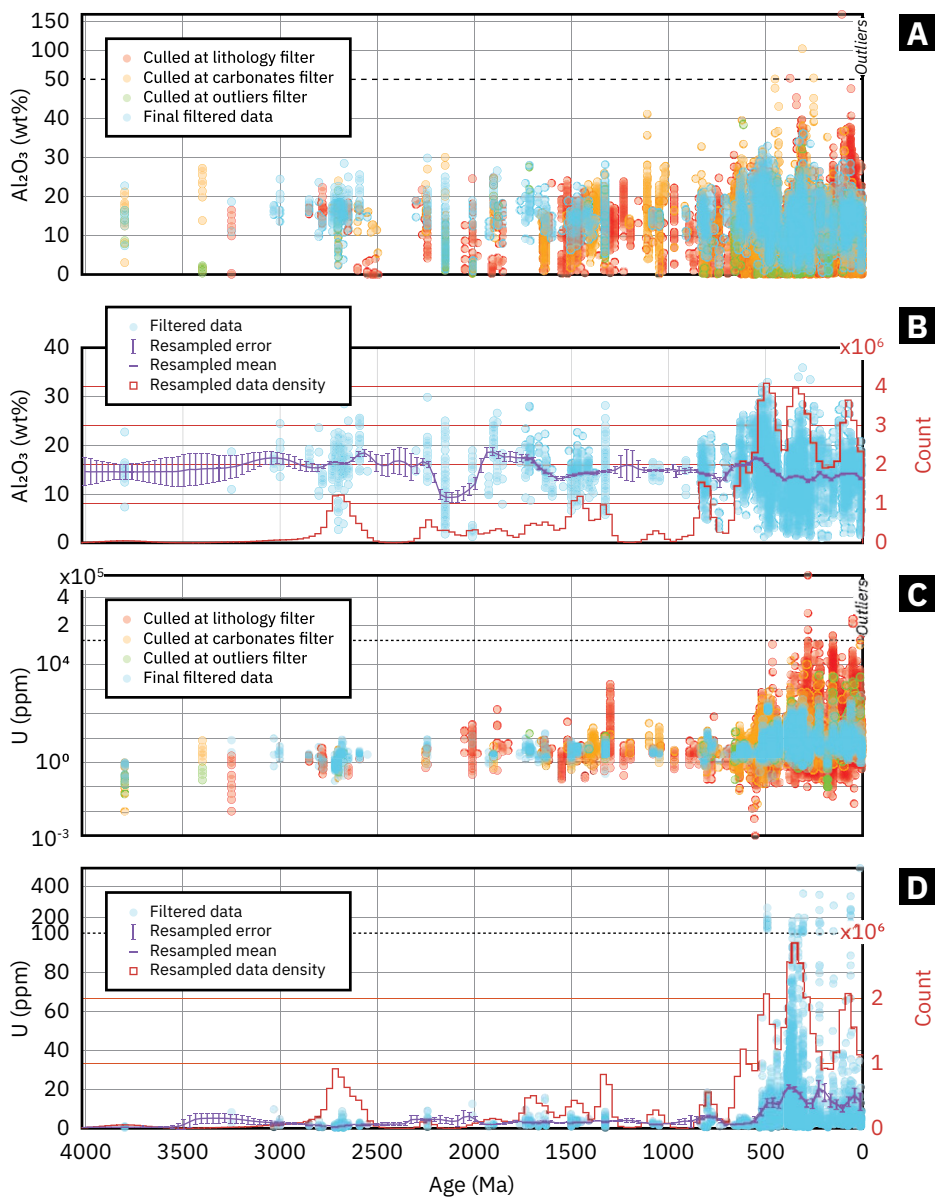


**Figure 2. Filtering and resampling of  $\text{Al}_2\text{O}_3$  and U. (A) and (C).  $\text{Al}_2\text{O}_3$  and U data through time, respectively. Each datum is color coded by the filtering step at which it was separated from the dataset. In blue is the final filtered data, which was used to generate the resampled trends in (B) and (D). (B) and (D). Plots depicting  $\text{Al}_2\text{O}_3$  and U filtered data, along with a histogram of resampled data density and the resulting resampled mean and  $2\sigma$  error. Note the log-scale y axis in (C).**

past ca. 1500 Ma (the time interval for which appreciable data exist in our dataset), suggesting little first-order change in  $\text{Al}_2\text{O}_3$  delivery to sedimentary basins over time. The U contents of mudstones shows a substantial increase between the Proterozoic and Phanerozoic. Although we have not accounted for the redox state of the overlying water column, these results broadly recapitulate the trends seen in a previous much smaller (and non-weighted) dataset (Partin et al., 2013) and generally may indicate oxygenation of the oceans within the Phanerozoic.

Moving forward, there is no reason to believe that the compilation and collection of published data, whether in a semi-automated (e.g., SGP) or automated (e.g., GeoDeepDive; Peters et al., 2014) manner, will slow and/or stop (Bai et al., 2017). Those interested in Earth's history—as collected in large compilations—should understand how to extract meaningful trends from these ever-evolving datasets. By presenting a workflow that is purposefully general and must be adapted before use, we hope to elucidate the various aspects that must be considered when processing large volumes of data.

**A** Foremost to any interpretation of a quantitative dataset is an assessment of uncertainty. In truth, a datum representing a physical quantity is not a single scalar point, but rather, an entire distribution. In many cases, such as in our workflow, this distribution is implicitly assumed to be Gaussian, an assumption that may or may not be accurate (Rock et al., 1987)—although a simplified distribution certainly is better than none. The quantification of uncertainty in Earth sciences especially is critical when averaging and binning by a selected independent variable, since neglecting the uncertainty of the independent variable will lead to interpretational failures that may not be mitigated by adding more data. As time perhaps is the most common independent variable (and one with a unique relationship to the assessment of causality), incorporating its uncertainty especially is critical for the purposes of Earth history studies (Ogg et al., 2016). An age without an uncertainty is not a meaningful datum. Indeed, such a value is even worse than an absence of data, for it is actively misleading. Consequently, assessment of age uncertainty is one of the most important, yet underappreciated, components of building accurate temporal trends from large datasets.

**B**

**C**

**D**

Of course, age is not the only uncertain aspect of samples in compiled datasets, and researchers should seek to account for as many inherent uncertainties as possible. Here, we propagate uncertainty by using a resampling methodology that incorporates information about space, time, and measurement error. Our chosen methodology—which is by no means the only option available to researchers studying large datasets—has the benefit of preventing one location or time range from dominating the resulting trend. For example, although the Archean records of  $\text{Al}_2\text{O}_3$  and U especially are sparse (Fig. 2), resampling prevents the appearance of artificial “steps” when transitioning from times with little data to instances of (relatively) robust sampling (e.g., see the resampled record of  $\text{Al}_2\text{O}_3$  between 4000 and 3000 Ma). Therefore, researchers should examine their selected methodologies to ensure that: (1) uncertainties are accounted for, and (2) spatiotemporal heterogeneities are addressed appropriately.

Even with careful uncertainty propagation, datasets must also be filtered to keep outliers from affecting the results. It is important to note that the act of filtering does not mean that the filtered data are necessarily “bad,” just that they do not meaningfully contribute to the question at hand. For example, while

our lithology and outlier filtering methods removed most U data because they were inappropriate for reconstructing trends in mudstone geochemistry through time, that same data would be especially useful for other questions, such as determining the variability of heat production within shales. This sort of filtering is a fixture of scientific research—e.g., geochemists will consider whether samples are diagenetically altered when measuring them for isotopic data—and, likewise, should be viewed as a necessary step in the analysis of large datasets.

As our workflow demonstrates, filtering often requires multiple steps, some automatic (e.g., cutoffs that exclude vast amounts of data in one fell swoop or algorithms to determine the “outlierness” of data; see Ptáček et al., 2020) and others manual (e.g., examining source literature to determine whether an anomalous value is, in fact, meaningful). Each procedure, along with any assumptions and/or justifications, must be documented clearly (and code included and/or stored in a publicly accessible repository) by researchers so that others may reproduce their results and/or build upon their conclusions with increasingly larger datasets.

Along with documentation of data processing, filtering, and sampling, it is important for researchers also to leverage sensitivity analyses to understand how parameter choices may impact resulting trends. Here, through the analysis of various spatial and temporal parameter values, we demonstrate that, while the spread of data varies based on the prescribed values of *scale<sup>spatial</sup>* and *scale<sup>temporal</sup>*, the averaged resampled trend does not (Fig. S7 [see footnote 1]). At the same time, we see that trends are directly influenced by the use (or lack thereof) of Ca and P<sub>2</sub>O<sub>5</sub> and outlier filtering. For example, the record of U in mudstones becomes overprinted by anomalously large values when carbonate samples are not excluded (Fig. S7B).

## CONCLUSIONS

Large datasets can provide increasingly valuable insights into the ancient Earth system. However, to extract meaningful trends, these datasets must be cultivated, curated, and processed with an emphasis on data quality, uncertainty propagation, and transparency. Charles Darwin once noted that the “natural geological record [is] a history of the world imperfectly kept” (Darwin, 1859, p. 310), a reality that is the result of both geological and sociological causes. But while the data are biased, they also are tractable. As

we have demonstrated here, the challenges of dealing with this imperfect record—and, by extension, the large datasets that document it—certainly are surmountable.

## ACKNOWLEDGMENTS

We thank everyone who contributed to the SGP database, including T. Frasier (YGS). BGS authors (JE, PW) publish with permission of the Executive Director of the British Geological Survey, UKRI. We would like to thank the editor and one anonymous reviewer for their helpful feedback.

## REFERENCES CITED

Algeo, T.J., and Li, C., 2020, Redox classification and calibration of redox thresholds in sedimentary systems: *Geochimica et Cosmochimica Acta*, v. 287, p. 8–26, <https://doi.org/10.1016/j.gca.2020.01.055>.

Bai, Y., Jacobs, C.A., Kwan, M., and Waldmann, C., 2017, Geoscience and the technological revolution [perspectives]: *IEEE Geoscience and Remote Sensing Magazine*, v. 5, no. 3, p. 72–75, <https://doi.org/10.1109/MGRS.2016.2635018>.

Chan, D., Kent, E.C., Berry, D.I., and Huybers, P., 2019, Correcting datasets leads to more homogeneous early-twentieth-century sea surface warming: *Nature*, v. 571, no. 7765, p. 393–397, <https://doi.org/10.1038/s41586-019-1349-2>.

Chen, L., and Wang, L., 2018, Recent advances in Earth observation big data for hydrology: *Big Earth Data*, v. 2, no. 1, p. 86–107, <https://doi.org/10.1080/20964471.2018.1435072>.

Darwin, C., 1859, *On the Origin of Species by Means of Natural Selection, or Preservation of Favoured Races in the Struggle for Life*: London, John Murray, 490 p.

Faghmous, J.H., and Kumar, V., 2014, A big data guide to understanding climate change: The case for theory-guided data science: *Big Data*, v. 2, no. 3, p. 155–163, <https://doi.org/10.1089/big.2014.0026>.

Gandomi, A., and Haider, M., 2015, Beyond the hype: Big data concepts, methods, and analytics: *International Journal of Information Management*, v. 35, no. 2, p. 137–144, <https://doi.org/10.1016/j.ijinfomgt.2014.10.007>.

Granitto, M., Giles, S.A., and Kelley, K.D., 2017, Global Geochemical Database for Critical Metals in Black Shales: U.S. Geological Survey Data Release, <https://doi.org/10.5066/F71G0K7X>.

IEEE, 2019, IEEE Standard for Floating-Point Arithmetic: IEEE Std 754-2019 (Revision of IEEE 754-2008), p. 1–84, <https://doi.org/10.1109/IEEESTD.2008.4610935>.

Keller, C.B., and Schoene, B., 2012, Statistical geochemistry reveals disruption in secular lithospheric evolution about 2.5 gyr ago: *Nature*, v. 485, no. 7399, p. 490–493, <https://doi.org/10.1038/nature11024>.

Nolet, G., 2012, *Seismic tomography: With applications in global seismology and exploration geophysics*: Berlin, Springer, v. 5, 386 p., <https://doi.org/10.1007/978-94-009-3899-1>.

Ogg, J.G., Ogg, G.M., and Gradstein, F.M., 2016, *A concise geologic time scale 2016*: Amsterdam, Elsevier, 240 p.

Partin, C.A., Bekker, A., Planavsky, N.J., Scott, C.T., Gill, B.C., Li, C., Podkovyrov, V., Maslov, A., Konhauser, K.O., Lalonde, S.V., Love, G.D., Poulton,

S.W., and Lyons, T.W., 2013, Large-scale fluctuations in Precambrian atmospheric and oceanic oxygen levels from the record of U in shales: *Earth and Planetary Science Letters*, v. 369, p. 284–293, <https://doi.org/10.1016/j.epsl.2013.03.031>.

Peters, S.E., and McClennen, M., 2016, The paleobiology database application programming interface: *Paleobiology*, v. 42, no. 1, p. 1–7, <https://doi.org/10.1017/pab.2015.39>.

Peters, S.E., Zhang, C., Livny, M., and Re, C., 2014, A machine reading system for assembling synthetic paleontological databases: *PLOS One*, v. 9, no. 12, e113523, <https://doi.org/10.1371/journal.pone.0113523>.

Peters, S.E., Husson, J.M., and Czaplowski, J., 2018, Macrostrat: A platform for geological data integration and deep-time Earth crust research: *Geochemistry Geophysics Geosystems*, v. 19, no. 4, p. 1393–1409, <https://doi.org/10.1029/2018GC007467>.

Potter, P.E., Maynard, J.B., and Depetris, P.J., 2005, *Mud and Mudstones: Introduction and Overview*: Berlin, Springer, 297 p.

Ptáček, M.P., Dauphas, N., and Greber, N.D., 2020, Chemical evolution of the continental crust from a data-driven inversion of terrigenous sediment compositions: *Earth and Planetary Science Letters*, v. 539, p. 116090.

Reinhard, C.T., Planavsky, N.J., Gill, B.C., Ozaki, K., Robbins, L.J., Lyons, T.W., Fischer, W.W., Wang, C., Cole, D.B., and Konhauser, K.O., 2017, Evolution of the global phosphorus cycle: *Nature*, v. 541, no. 7637, p. 386–389, <https://doi.org/10.1038/nature20772>.

Rock, N.M.S., Webb, J.A., McNaughton, N.J., and Bell, G.D., 1987, Nonparametric estimation of averages and errors for small data-sets in isotope geoscience: A proposal: *Chemical Geology, Isotope Geoscience Section*, v. 66, no. 1–2, p. 163–177.

Sarbas, B., 2008, The Georoc database as part of a growing geoinformatics network, *in* *Geoinformatics 2008—Data to Knowledge*: U.S. Geological Survey, p. 42–43.

Schoene, B., 2014, U-Th-Pb geochronology, *in* *Holland, H.D., and Turekian, K.K., eds., Treatise on Geochemistry (Second Edition)*: Oxford, UK, Elsevier, p. 341–378.

Sperling, E.A., Tecklenburg, S., and Duncan, L.E., 2019, Statistical inference and reproducibility in geobiology: *Geobiology*, v. 17, no. 3, p. 261–271, <https://doi.org/10.1111/gbi.12333>.

Walker, J.D., Lehnert, K.A., Hofmann, A.W., Sarbas, B., and Carlson, R.W., 2005, EarthChem: International collaboration for solid Earth geochemistry in geoinformatics: *AGUFM*, v. 2005, IN44A-03.

Woodcock, N.H., 2004, Life span and fate of basins: *Geology*, v. 32, no. 8, p. 685–688, <https://doi.org/10.1130/G20598.1>.

Young, G.M., and Nesbitt, H.W., 1998, Processes controlling the distribution of Ti and Al in weathering profiles, siliciclastic sediments and sedimentary rocks: *Journal of Sedimentary Research*, v. 68, no. 3, p. 448–455.

MANUSCRIPT RECEIVED 28 SEPT. 2020

REVISED MANUSCRIPT RECEIVED 2 DEC. 2020

MANUSCRIPT ACCEPTED 20 FEB. 2021